Analysis of hole-like traps in deep level transient spectroscopy spectra of AlGaN/GaN heterojunctions

Philippe Ferrandis, Matthew Charles, Marc Veillerot, Charlotte Gillot

Analysis of hole-like traps in deep level transient spectroscopy spectra of AlGaN/GaN heterojunctions

Philippe Ferrandis[1,2,*], Matthew Charles[2], Marc Veillerot[2] and Charlotte Gillot[2]

[1]Université de Toulon, Univ. Grenoble Alpes, CNRS, Institut Néel, 38000 Grenoble, France
[2]Univ. Grenoble Alpes, CEA, LETI, 38000 Grenoble, France

* email: philippe.ferrandis@univ-tln.fr

Abstract

When a hole-like trap appears in deep level transient spectroscopy spectra of devices with an AlGaN/GaN heterojunction, surface states at the top of the AlGaN layer are often incriminated. However, no deep investigation has proved that this anomalous signal is related to interface states. In this work, we made a full study of a hole-like signal which appears in spectra of AlGaN/GaN Schottky barrier diodes. The mechanism responsible for the formation of the peak is determined, a model is proposed and this is then applied to make our analysis. We show that two deep donor levels in the AlGaN layer are responsible for the formation of the hole-like signal and we have determined their activation energies and their concentrations. With the help of secondary ion mass spectrometry studies, the dominant trap was assigned to a nitrogen antisite defect, which is in accordance with the literature. The second trap was tentatively associated with gallium vacancy related defects. The mechanism responsible for the formation of the hole-like signal allows the loss of electrons in the channel of the diode to be understood, and the amplitude of the peak is a way to quantify the importance of this loss.

I. Introduction

The AlGaN/GaN heterostructure has been demonstrated to be a promising candidate for high power amplifiers in the microwave communication system and high-voltage power switches [1-4]. The combination of GaN device performance with the low cost of silicon substrates enhances the interest of this technology. Despite numerous improvements of GaN power components during the last decades, charge trapping effects at deep levels still lead to dynamic on-resistance and switching losses [5-7]. To detect these deep traps and determine in which part of the device structure they are located, capacitance deep level transient spectroscopy (DLTS) has been applied to GaN Schottky barrier diodes (SBDs) [8-11].

Hole-like traps are frequently observed in DLTS spectra of devices with n-type AlGaN/GaN heterojunctions without any minority carriers. Many works refer to previous studies carried out in AlGaAs/GaAs systems to explain the nature of these DLTS signals [12-14]. Hence, hole-like traps are often associated with surface states at the ungated SiN/AlGaN interface [15-18]. They are sometimes related to bulk traps in the AlGaN layer [19, 20] or to the transfer of electrons by tunneling effect from the traps in the lower half of the AlGaN bandgap into the states in the GaN buffer [21, 22].

To our knowledge, no deep investigation exists to clearly identify the origin of hole-like traps in AlGaN/GaN heterojunctions. A detailed understanding of the trapping mechanism involved in this anomalous DLTS signal is of fundamental importance to learn which defects affect device performance such as the gate-lag, for instance [20]. This work is focused on the study of a hole-like signal which appears in DLTS spectra of AlGaN/GaN SBDs.

II. Experimental methods

SBDs were produced on structures grown by metalorganic chemical vapor deposition on 200 mm diameter Si(111) substrates. The epitaxy consists of an AlN nucleation layer, followed by 1.6 µm AlGaN buffer layers, then a 1.6 µm thick semi-insulating carbon doped GaN buffer layer, a 100 nm unintentionally doped (UID) GaN layer acting as the channel, an UID AlN spacer and an UID AlGaN barrier layer, completed by SiN passivation. Two structures (A and B) were processed into diodes with a summary of the key physical parameters around the active region shown in Table I.

SBD name	AlGaN thickness (nm)	Al content in AlGaN (%)	AlN thickness (nm)	Ammonia partial pressure
A	24.1	25	1	Low
B	24.1	22.5	0.7	High

Table I : Features of AlGaN and AlN layers in structures A and B.

Interdigitated comb-like diodes with twenty-six 15 x 1000 µm^2 fingers were then formed using TiN/W as Schottky electrodes and Ti/Al annealed for 30 s at 875 °C as Ohmic contacts. Recessed Schottky electrodes were achieved by etching the SiN passivation, the AlGaN/AlN bilayer and 6 nm of the GaN layer using a low bias chlorine (Cl_2/BCl_3) etching process with Inductively Coupled Plasma - Reactive Ion Etching [23]. A schematic of SBDs can be seen in figure 1. For all diodes, the Schottky/Ohmic spacing is 15 µm and the Schottky electrode has 0.5 µm long field plates which cover 30 nm of SiN.

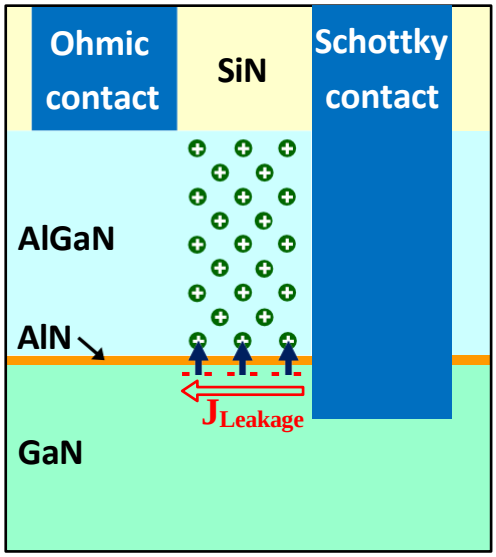

Figure 1 : Schematic of Schottky barrier diodes produced. See the text in section VI and VII for the explanation on the charge transfer.

Capacitance data were acquired with a DLTS system using a Boonton 7200 capacitance meter with a 100 mV test signal at 1 MHz. Capacitance transients were recorded in the warm up mode but no difference was observed with the cool down mode. Current-voltage measurements were carried out with a Keithley 238 source measure unit.

III. Secondary ion mass spectrometry analysis

During the growth, the increase of the ammonia partial pressure results in a higher incorporation of nitrogen atoms, which leads to a reduction of nitrogen vacancies (V_N). As carbon atoms tend to incorporate preferentially to V_N sites [24], the carbon concentration decreases when the ammonia partial pressure rises.

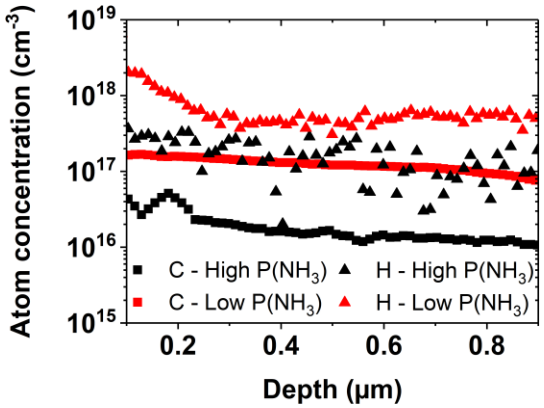

Figure 2 : SIMS profile of carbon and hydrogen atoms in AlGaN layers made with a low and high ammonia partial pressure P(NH_3).

Figure 2 reports the secondary ion mass spectrometry (SIMS) profile of carbon and hydrogen atoms concentration in AlGaN layers formed with the same ammonia partial pressures that those used to carry out AlGaN barriers of diodes A and B. With the high ammonia partial pressure (SBD B), the carbon concentration is reduced by one order of magnitude. SIMS experiments did not reveal any difference between the two AlGaN layers for Si and O atoms. However, the concentration of H atoms was slightly higher in the AlGaN performed with a lower ammonia partial pressure (SBD A).

IV. Static measurements

Figure 3 reports capacitance-voltage (C-V) measurements of SBDs A and B at room temperature.

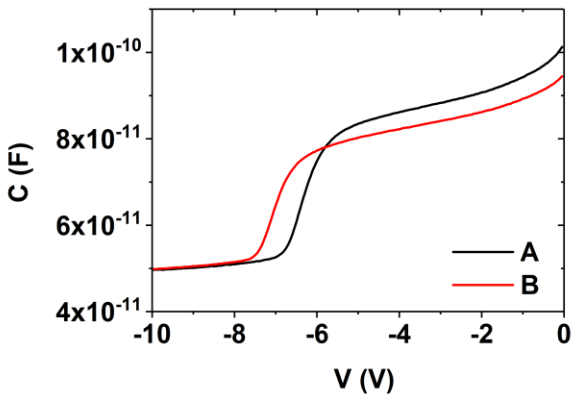

Figure 3 : Capacitance-voltage characteristic of diodes A and B carried out at room temperature and 1 MHz.

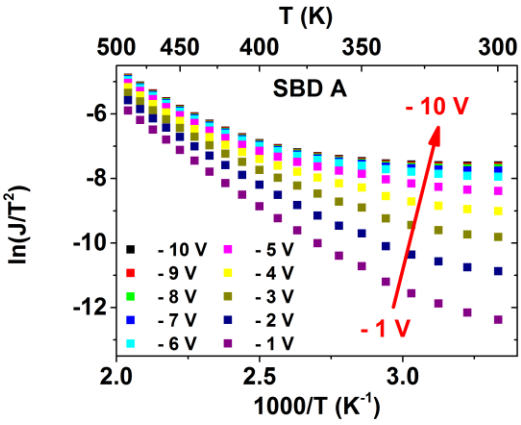

Figure 4 : Evolution with the temperature of the reverse current density (A.m^{-2}) of diode A over the square of the temperature.

We see that the channel is pinched-off at – 6.8 V and – 7.5 V for diodes A and B, respectively. When the reverse voltage is below these values, the capacitance is equivalent to two capacitances in series associated with the AlGaN-barrier and the SiN insulator located below the field plates. As soon as the pinch-off voltage is reached, the 2DEG is completely depleted underneath the field plates and the capacitance of the diode strongly decreases to a value related to the piezoelectric charge at the AlGaN/GaN interface.

The reverse current of the diodes was measured as a function of the voltage until – 10 V and the temperature between 300 K and 500 K. Above 430 K, the reverse leakage current density of diodes A (figure 4) and B follows the relation [25, 26]

$$J = a\,T^2\,exp\,(-\frac{\phi_b}{K\,T}) \qquad (1)$$

where J is the reverse leakage current density of the diode, a is a constant, T is the temperature, Φ_b is the thermal barrier height and K is the Boltzmann's constant.

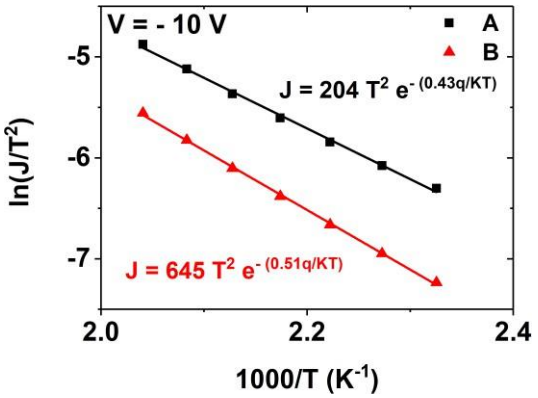

Figure 5 : Linear fit (straight lines) of experimental data points (scatters) for SBDs A and B. The current density J is expressed in A.m^{-2}.

Parameters a and Φ_b have been determined by a linear fit of experimental data points in the plot $\ln(J/T^2)$ as a function of $1/T$ for diodes A and B at – 10 V (figure 5). SBD A has a higher current density, which results from a lower barrier height at 0.43 ± 0.01 eV compared to 0.51 ± 0.01 eV for diode B.

In figure 4, we remark that the current is almost identical for a voltage between – 7 V and – 10 V. In this range of bias, we see in figure 3 that the channel is pinched off. Consequently, the number of electrons in the channel does not change any further with the applied voltage and the current saturates.

V. DLTS study

Figure 6 reports DLTS spectra of diodes A and B recorded with a reverse bias V_R = – 10 V, a filling pulse height V_P = – 2 V, a filling pulse width t_P = 10 ms and a rate window R_W = 10 Hz. A hole-like signal centered at 442 K for both devices dominates the spectra. The amplitude of this

peak is 20 % larger for SBD B, nevertheless this level is expected to have the same origin in both diodes. By changing the reverse bias between – 8 V and – 10 V, keeping V_P = – 2 V, a slight increase of the low temperature part of the peak takes place (figure 7).

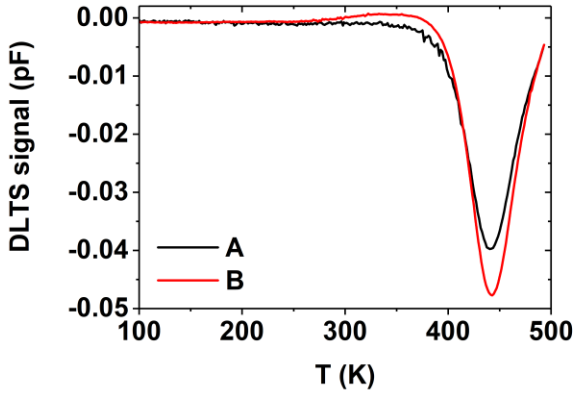

Figure 6 : DLTS spectra of diodes A and B recorded with V_R = – 10 V, V_P = – 2 V, t_P = 10 ms and R_W = 10 Hz.

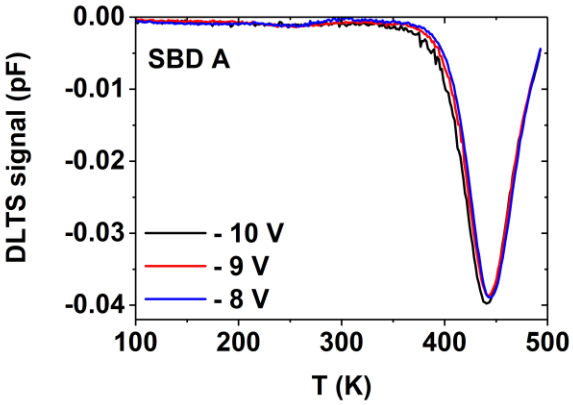

Figure 7 : DLTS spectra of diode A recorded with V_P = – 2 V, t_P = 10 ms, R_W = 10 Hz and V_R varying between – 10 V and – 8 V.

However, a variation of the filling pulse height between – 3 V and – 1 V, keeping V_R = – 10 V, leads to an increase of the amplitude and the low temperature part of the peak (figure 8). Consequently, the position of the hole-like signal shifts towards lower temperatures. A study with rate windows ranging between 10 Hz and 200 Hz allowed extracting the apparent activation energy related to the peak. Arrhenius plots performed with a filling pulse width of 10 ms are introduced in figure 9.

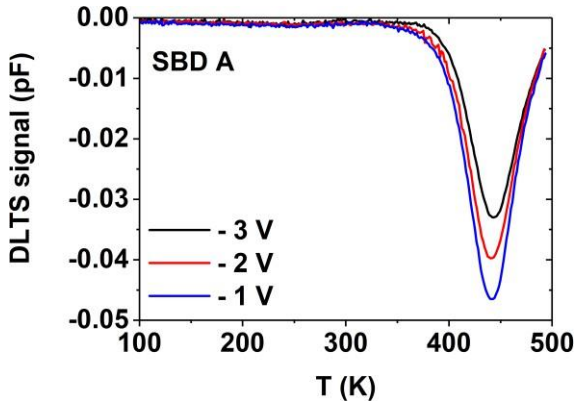

Figure 8 : DLTS spectra of diode A recorded with V_R = – 10 V, t_P = 10 ms, R_W = 10 Hz and V_P varying between – 3 V and – 1 V.

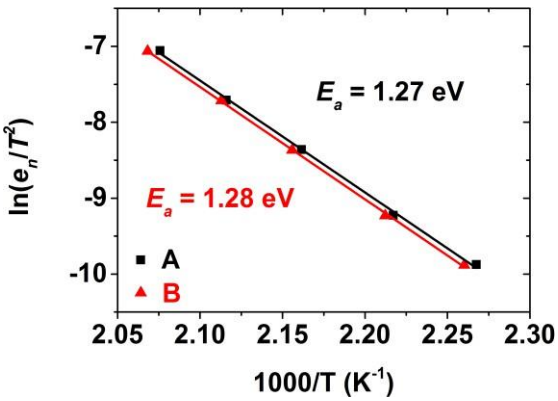

Figure 9 : Arrhenius plots used to extract the apparent activation energies of the hole-like trap with diodes A and B. Data were recorded with V_R = – 10 V, V_P = – 2 V and t_P = 10 ms.

As no minority carriers are expected in the GaN layer probed by DLTS, we have therefore to understand the physical meaning of this apparent activation energy and to explain the behavior of the hole-like signal with the change of the reverse and filling voltages.

VI. Hole-like signal mechanism

In figure 10, the DLTS signal undergoes a significant change when the rate window rises. The large increase of the peak height cannot be explained by considering only the thermal emission rate of a trap [26, 27]. A similar increase of the peak height and the reverse leakage current of the diode has been noted when the temperature rises (figure 11). A link is then likely between the emission process responsible for the hole-like trap and the arrival in the channel of electrons coming from the Schottky electrode. Furthermore, a saturation of the peak height appears with $t_P \geq 50$ ms for high temperatures i.e. high rate windows.

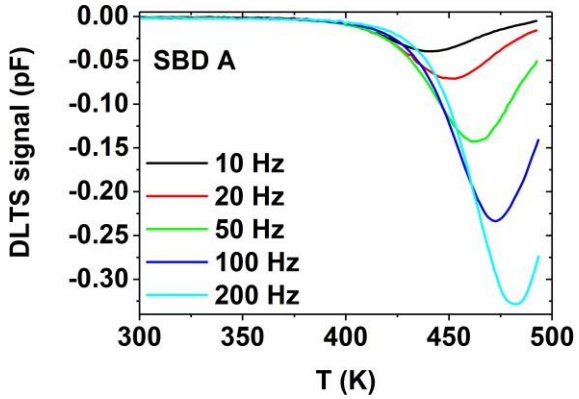

Figure 10 : DLTS spectra of diode A recorded with V_R = – 10 V, V_P = – 2 V, t_P = 10 ms and R_W varying between 10 Hz and 200 Hz.

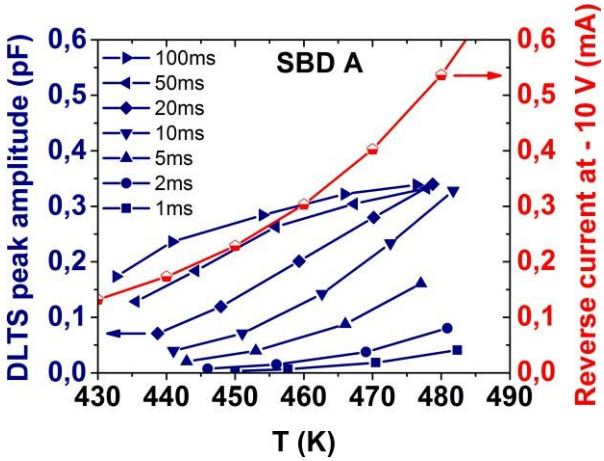

Figure 11 : DLTS peak amplitude (Left axis) versus temperature, collected from spectra obtained using V_R = – 10 V, V_P = – 2 V, R_W = 10 Hz and t_P varying between 1 ms and 100 ms. Reverse leakage current of the diode at – 10 V (Right axis) as a function of the temperature. Results introduced in this figure are for diode A.

When V_P is applied, the Fermi level is close to the conduction band minimum of the AlGaN layer. Hence, the electrons of the two-dimensional electron gas (2DEG) have a higher probability to be transferred towards the AlGaN layer (blue vertical arrows in figure 1) to neutralize donor traps that were initially positively charged [28] (green circles with white crosses in figure 1). This process is slow because the carriers must cross over the AlN layer by tunneling. Even if the tunnel time to cross a barrier is expected to be in the femtosecond range [29], the flow of the electrons which follow this way is small because the electric field in the channel does not favor this path. Moreover, the AlN layer is added in the structure of the diode to reduce the leakage of electrons towards the AlGaN layer [30]. The flow of the electrons which cross the AlN layer is then expected to be small. During the filling pulse, the quantity of electrons in the 2DEG is therefore reduced, making believe to holes capture in the channel. When the system returns to V_R, if the temperature is enough high, the electrons trapped in donor states are thermally emitted towards the AlGaN conduction band. The reverse leakage current can then refill the 2DEG (red horizontal arrow in figure 1) and a negative DLTS peak corresponding to holes emission appears in the spectra. This anomalous signal is therefore a reflection of trapping occurring in the AlGaN layer and its study allows obtaining features of the donor states.

VII. Discussions

A. Determination of trap features

The change of the peak shape, which leads to a shift of the maximum towards low temperatures when V_P increases from – 3 V to – 1 V (figure 8), indicates that donor states are bulk deep levels with dependence of the emission rate on the electric field [31]. This feature is also supported by the increase of the low temperature part of the peak when V_R is changed from – 8 V to – 10 V (figure 7) [31].

Furthermore, the thickness of the AlN film is 1 nm and 0.7 nm in SBDs A and B, respectively (Table I). Electrons have therefore to cross over a thicker barrier to reach traps in the AlGaN layer with diode A. Thus, for the same pulse duration, fewer electrons are captured and the peak amplitude is reduced (figure 6).

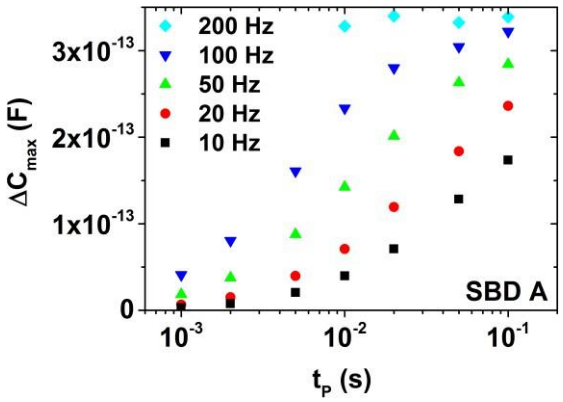

Figure 12 : Amplitude of the DLTS peak versus the pulse duration for diode A. Results comes from spectra realized with V_R = – 10 V, V_P = – 2 V and R_W varying between 10 Hz and 200 Hz.

In figure 12, the amplitude of the DLTS peak is plotted as a function of the filling pulse width. We observe a delay before the DLTS peak grows which corresponds to the time needed by electrons to cross the tunnel barrier formed by the AlN film. The saturation of the amplitude as a function of ln(t_P) allows us to conclude that traps in the AlGaN responsible for the hole-like signal are point defects instead of extended defects [32].

The DLTS signal is expressed by [33]

$$S(T) = \Delta C(0)\ [e^{-(\frac{t_1}{\tau})} - e^{-(\frac{t_2}{\tau})}] \qquad (2)$$

where $\Delta C(0)$ is the capacitance change due to the pulse at t = 0, t_1 and t_2 are the times of the double boxcar method which define the rate window R_W and τ is the transient time constant.

In the channel, a hole emission is related to the capture of an electron coming from the Schottky electrode by the reverse leakage current. The transient time constant τ therefore represents the capture rate of electrons in the channel. The limiting mechanism is the emission of trapped electrons by donor states in AlGaN. An electron comes into the channel and produces the

disappearance of a hole only if a trapped electron in AlGaN is thermally emitted. Thus, the inverse of the transient time constant depends on the reverse leakage current density J (equation 1) and the capture cross section of electrons in the GaN channel which is related to the emission of the electrons located on trap x in the AlGaN barrier [26, 27].

$$\tau^{-1} = \frac{J \Sigma \sigma_x}{q} \tag{3}$$

q is the electronic charge.

The capture cross section σ_x depends on the emission rate of the electrons localized on trap x which is thermally activated [34]. Therefore σ_x can be expressed by the following equation.

$$\sigma_x = c_x \, exp\left(-\frac{\phi_{\sigma x}}{K\,T}\right) \tag{4}$$

c_x is a constant and $\Phi_{\sigma x}$ is the thermal ionization energy of electrons which fill donor state x in the AlGaN layer.

The apparent activation energy E_a which characterizes the evolution of τ^{-1} with the temperature is consequently the sum of Φ_b and $\Phi_{\sigma x}$.

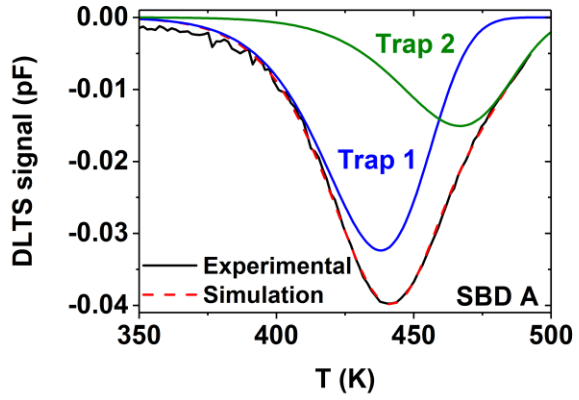

Figure 13 : Simulation using equations 2-4 of the experimental DLTS spectrum of diode A shown in Fig. 6.

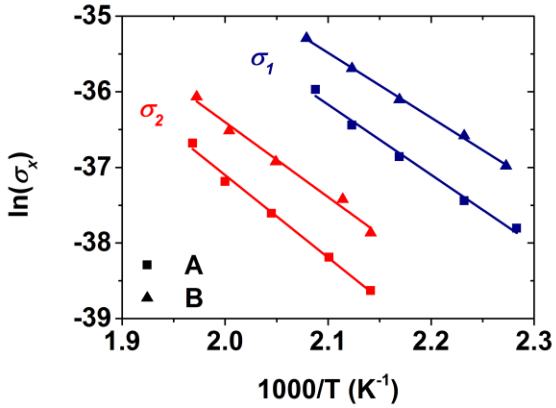

Figure 14 : Evolution of the capture cross section of traps 1 and 2 found by the simulations of DLTS spectra as a function of the inverse of the temperature for diodes A and B (scatters). Results are shown for t_P = 10 ms. Solid lines are linear fits of data points.

The simulation of the DLTS spectra shown in figure 6 using equations 2-4 demonstrates that two traps are involved in the hole-like peak (figure 13). All spectra carried out with five rate windows ranging from 10 Hz to 200 Hz were simulated. Both electron capture cross sections σ_1 and σ_2 exhibit a linear dependence on the inverse of the temperature in a logarithm scale (figure 14). The slope of these plots allows the values of $\Phi_{\sigma 1}$ and $\Phi_{\sigma 2}$ to be deduced.

Table II summarizes data with t_P = 10 ms of E_a, for both diodes, extracted from experimental Arrhenius plots (figure 9), with $E_a - \Phi_b$ (see figure 5 for Φ_b), $\Phi_{\sigma 1}$ and $\Phi_{\sigma 2}$ determined from plots of $\ln(\sigma_x)$ versus 1000/T (figure 14).

SBD	E_a (eV)	$E_a - \Phi_b$ (eV)	$\Phi_{\sigma 1}$ (eV)	$\Phi_{\sigma 2}$ (eV)	N_{t1} (cm^{-3})	N_{t2} (cm^{-3})
A	1.27 ± 0.03	0.84 ± 0.04	0.80 ± 0.04	0.94 ± 0.04	4.1×10^{13}	1.9×10^{13}
B	1.28 ± 0.01	0.77 ± 0.02	0.74 ± 0.02	0.85 ± 0.06	5.3×10^{13}	2.3×10^{13}

Table II : For t_P = 10 ms, values of E_a, $E_a - \Phi_b$, the thermal activation energy Φ_σ and the concentration N_t of traps 1 and 2 in SBDs A and B, respectively.

According to the above model, $\Phi_{\sigma 1}$ and $\Phi_{\sigma 2}$ represent the thermal activation energies with respect to the conduction band minimum of two donor states located in the AlGaN layer. Comparing both diodes, we notice a reduction in energy of 0.06-0.09 eV for $\Phi_{\sigma 1}$ and $\Phi_{\sigma 2}$ in diode B. This difference is explained by the aluminum content of the AlGaN layers (Table I). The band offsets for AlGaN on GaN is ΔE_C (Al = 0.25) = 0.466 eV and ΔE_C (Al = 0.225) = 0.391 eV for diodes A and B, respectively [35]. The difference of 0.075 eV is responsible for the difference observed on the energies $\Phi_{\sigma 1}$ or $\Phi_{\sigma 2}$ between the SBDs. Thus, it is reasonable to conclude that the two traps have the same origin in both diodes as suggested by the results in figure 6.

The emission of electrons towards the AlGaN layer during the filling pulse and the providing of charge by the reverse leakage current when returning to the reverse voltage change the width of the space charge region in GaN layers. Thus, the capacitance of the diode in depletion follows these variations of charge. The quantity of traps can therefore be estimated by the relation [33, 36]

$$N_t = \frac{\Delta C_{sat}}{C_R} \; 2\, N_{CV} \tag{5}$$

where N_t is the concentration of traps, ΔC_{sat} is the amplitude of the DLTS peak at saturation and C_R is the capacitance of the diode at V_R.

N_{CV} is the effective doping level of the GaN layer in depletion determined by means of C-V measurements with [37]

$$N_{CV} = \frac{C^3}{q\, \varepsilon_0\, \varepsilon} \frac{dV}{dC} \tag{6}$$

where C is the measured diode capacitance per unit area, V is the voltage applied to the Schottky contact, ε_0 and ε are the dielectric constants of the vacuum and the GaN material, respectively.

N_{CV} was found at 3.67×10^{15} cm^{-3} and 3.8×10^{15} cm^{-3} for diodes A and B, respectively and C_R was measured at 4.96×10^{-11} F. The DLTS peak saturates at $\Delta C_{max} = 3.37\times10^{-13}$ F (figures 11 and 12) and $\Delta C_{max} = 4.03\times10^{-13}$ F for diodes A and B, respectively. The simulation of the hole-like signals at saturation yields the maxima of each trap $\Delta C_{sat}1$ and $\Delta C_{sat}2$. Equation (5) allows these values to be converted to trap concentrations. It is clear from the results summarized in Table II that the density of trap 1 is higher in SBD B than in SBD A whereas the concentration of trap 2 is

approximatively the same in both diodes. N_{t1} and N_{t2} are average values with a variation of $\pm 0.1\times10^{13}$ cm^{-3} determined using the simulation of several peaks in the saturated part of figure 11.

B. Identification of the traps

Using DLTS, Götz *et al.* [38] found a dominant deep donor in $Al_{0.12}Ga_{0.88}N$ with an activation energy for electron emission to the conduction band of 0.61 eV. The activation energy of this level displays a pronounced field dependence. As suggested by Götz *et al.* [38], it is likely that the level found in $Al_{0.12}Ga_{0.88}N$ is the same in GaN (E2 in [8], D2 in [39], DLN3 in [40], B in [41]), which has been attributed to nitrogen antisite N_{Ga} [39]. Zhu *et al.* [15] reported a level at E_C – 0.88 eV in $Al_{0.3}Ga_{0.7}N$ and assigned it to N_{Ga}. Therefore, trap 1 found at E_C – 0.8 eV in $Al_{0.25}Ga_{0.75}N$ and E_C – 0.74 eV in $Al_{0.225}Ga_{0.775}N$ agrees well with N_{Ga} defects.

Our SIMS measurements allow C or H related defects to be ruled out as a possible origin for traps 1 and 2 since their concentrations are larger in SBD A. However, more incorporation of N atoms is expected in SBD B due to the larger partial pressure of ammonia used to carry out the AlGaN layer. The association of trap 1 to N_{Ga} defects is thus consistent with SIMS results. In addition, the nitrogen antisite has already been detected in GaN grown with our epitaxial chamber [42-45]. It is thus very likely to find it in the AlGaN layer.

Finally, we believe that trap 1 is similar with the reported levels ranging between 0.7 eV and 0.9 eV in $Al_{0.25}Ga_{0.75}N$ [20, 28, 46] and is responsible for the hole-like trap reported at 1.24-1.3 eV in AlGaN/GaN SBDs [19].

Trap 2 has a thermal activation energy 0.11-0.14 eV larger than trap 1 and its amplitude is approximatively the same for both diodes. It is likely that trap 2 is related to a native defect which does not involve C, H and N atoms. Assuming that the energy difference between the levels related to traps 1 and 2 are similar in AlGaN and GaN materials, trap 2 could be associated with Ga vacancy (V_{Ga}) related defects [8, 39, 41, 42, 47-49].

VIII. Conclusions

This work introduces a deep study on a hole-like signal which appears in DLTS spectra of AlGaN/GaN SBDs. A correlation between the amplitude of the peak and the reverse leakage current of the diode has been demonstrated and a mechanism is proposed to explain the formation of the hole-like signal. During the pulse voltage, electrons move by tunneling conduction from the 2DEG towards the AlGaN layer where they are captured on deep donor states. When the temperature is increased and the reverse voltage is applied on the anode, the thermal energy removes electrons from the traps and the 2DEG is refilled by the reverse leakage current of the diode. The hole-like signal results from the return of electrons into the 2DEG. The simulation of the DLTS peak using a model involving a transient time constant, which takes into account the thermal activation energy of the reverse leakage current of the diode, leads to the extraction of two deep levels in AlGaN. The concentration of the dominant trap depends on the ammonia partial pressure used to perform the AlGaN layer and was calculated at $4.1\text{x}10^{13}$ cm^{-3} and $5.3\text{x}10^{13}$ cm^{-3} for SBDs A and B, respectively. This trap was assigned to nitrogen antisite defects. The second trap was tentatively associated with Ga vacancy related defects. The proposed model allows an explanation of the origin of traps reported in the literature. In addition, this work demonstrates that information can be extracted from a hole-like signal in AlGaN/GaN heterojunctions to access features of traps in AlGaN. We also demonstrated that the amplitude of the hole-like signal is an indication of the quantity of electrons which leave the 2DEG. Since the reduction of electrons in the 2DEG directly results in a decrease of device performance, the

appearance of a hole-like signal in DLTS spectra of AlGaN/GaN heterojunctions should be thoroughly investigated.

Acknowledgments
This work was funded by the French national program "programme d'Investissements d'Avenir, IRT Nanoelec" ANR-10-AIRT-05. Thanks to Charles Leroux for helpful discussions.

References
[1] U. K. Mishra, L. Shen, T. E. Kazior, and Y. F. Wu, Proc. IEEE 96, 287 (2008).
[2] T. Kikkawa, K.Makiyama, T. Ohki,M. Kanamura, K. Imanishi, N. Hara, K. Joshin, Phys. Status Solidi A 206, 1135 (2009).
[3] N. Ikeda, Y. Niiyama, H. Kambayashi, Y. Sato, T. Nomura, S. Kato, and S. Yoshida, Proc. IEEE 98, 1151 (2010).
[4] E. A. Jones, F. Wang, and D. Costinett, IEEE J. Emerg. Sel. Topics Power Electron 4, 707 (2016).
[5] R. Vetury, N.-Q. Zhang, S. Keller, U.K. Mishra, IEEE Trans. Electron Devices 48, 560 (2001).
[6] P. B. Klein, J. A. Freitas Jr., S. C. Binari, A. E. Wickenden, Appl. Phys. Lett. 75, 4016 (1999).
[7] M. Meneghini, N. Ronchi, A. Stocco, G. Meneghesso, U. K. Mishra, Y. Pei, E. Zanoni, IEEE Trans. Electron Devices 58, 2996 (2011).
[8] P. Hacke, T. Detchprohm, K. Hiramatsu, N. Sawaki, K. Tadatomo and K. Miyake, J. Appl. Phys. 76, 304 (1994).
[9] W. Götz, N. M. Johnson, H. Amano and I. Akasaki, Appl. Phys. Lett. 65, 463 (1994).
[10] P. Hacke, H. Nakayama, T. Detchprohm, K. Hiramatsu and N. Sawaki, Appl. Phys. Lett. 68, 1362 (1996).
[11] W. Götz, N. M. Johnson and D. P. Bour, Appl. Phys. Lett. 68, 3470 (1996).
[12] S. R. Blight, R. H. Wallis and H. Thomas, IEEE Trans. Electron Devices ED-33,1447 (1986).
[13] K. J. Choi and J.-L. Lee, J. Vac. Sci. Technol. B 19, 615 (2001).
[14] A. Cavallini, G. Verzellesi, A. F. Basile, C. Canali, A. Castaldini, and E. Zanoni, J. Appl. Phys. 94, 5297 (2003).
[15] Q. Zhu, X.-H. Ma, W.-W. Chen, B. Hou, J.-J. Zhu, M. Zhang, L.-X. Chen, Y.-R. Cao and Y. Hao, Chin. Phys. B 25, 067305 (2016).
[16] J. K. Kaushik, V. R. Balakrishnan, D. Mongia, U. Kumar, S. Dayal, B. S. Panwar, R. Muralidharan, Thin Solid Films 612, 147 (2016).
[17] T. Mizutani, T. Okino, K. Kawada, Y. Ohno, S. Kishmoto, and K. Maezawa, Phys. Status Solidi A 200, 195 (2003).
[18] T. Okino, M. Ochiai, Y. Ohno, S. Kishimoto, K. Maezawa, and T. Mizutani, IEEE Electron Device Lett. 25, 523 (2004).
[19] Z.-Q. Fang, B. Claflin, D. C. Look, D. S. Green and R. Vetury, J. Appl. Phys. 108, 063706 (2010).
[20] A. Y. Polyakov, N. B. Smirnov, I. V. Shchemerov, Fan Ren and S. J. Pearton, ECS J. Solid State Sci. Technol. 6, S3034 (2017).
[21] A. Y. Polyakov and I.-H. Lee, Mater. Sci. Eng. R 94, 1 (2015).
[22] K. L. Enisherlova, Yu. V. Kolkovskii, E. A. Bobrova, E. M. Temper and S. A. Kapilin, Russ. Microelectron. 48, 28 (2019).

[23] P. Ferrandis, M. Charles, Y. Baines, J. Buckley, G. Garnier, C. Gillot and G. Reimbold, Jpn. J. Appl. Phys. 56, 04CG01 (2017).
[24] J. L. Lyons, A. Janotti and C. G. Van de Walle, Phys. Rev. B 89, 035204 (2014).
[25] F. Hasegawa, M. Onomura, C. Mogi and Y. Nannichi, Solid State Electron. 31, 223 (1988).
[26] K. Dmowski, B. Lepley, E. Losson and M. El Bouabdellati, J. Appl. Phys. 74, 3936 (1993).
[27] M. C. Chen, D. V. Lang, W. C. Dautremont-Smith, A. M. Sergent and J. P. Harbison, Appl. Phys. Lett. 44, 790 (1984).
[28] T.-L. Wu, D. Marcon, N. Ronchi, B. Bakeroot, S. You, S. Stoffels, M. Van Hove, D. Bisi, M. Meneghini, G. Groeseneken, S. Decoutere, Solid State Electron. 103, 127 (2015).
[29] P. Février and J. Gabelli, Nat Commun 9, 4940 (2018).
[30] S. W. Kaun, M. H. Wong, U. K. Mishra and J. S. Speck, Appl. Phys. Lett. 100, 262102 (2012)
[31] A. V. P. Coelho, M. C. Adam and H. Boudinov, J. Phys. D: Appl. Phys. 44, 305303 (2011).
[32] T. Wosiński, J. Appl. Phys. 65, 1566 (1989).
[33] D. V. Lang, J. Appl. Phys. 45, 3023 (1974).
[34] P. Blood and J. W. Orton, Techniques of Physics 14, The Electrical Characterization of Semiconductors: Majority Carriers and Electron States, Academic press 1992, p.344
[35] D. R. Hang, C. H. Chen, Y. F. Chen, H. X. Jiang and J. Y. Lin, J. Appl. Phys. 90, 1887 (2001).
[36] M. Musolino, D. van Treeck, A. Tahraoui, L. Scarparo, C. De Santi, M. Meneghini, E. Zanoni, L. Geelhaar and H. Riechert, J. Appl. Phys. 119, 044502 (2016).
[37] O. Ambacher, J. Smart, J. R. Shealy, N. G. Weimann, K. Chu, M. Murphy, W. J. Schaff, L. F. Eastman, R. Dimitrov, L. Wittmer, M. Stutzmann, W. Rieger, and J. Hilsenbeck, J. Appl. Phys. 85, 3222 (1999).
[38] W. Götz, N. M. Johnson, M. D. Bremser and R. F. Davis, Appl. Phys. Lett. 69, 2379 (1996).
[39] D. Haase, M. Schmid, W. Kürner, A. Dörnen, V. Härle, F. Scholz, M. Burkard and H. Schweizer, Appl. Phys. Lett. 69, 2525 (1996).
[40] W. Götz, J. Walker, L. T. Romano, N. M. Johnson and R. J. Molnar, Mat. Res. Soc. Symp. Proc. 449, 525 (1997).
[41] Z-Q. Fang, D. C. Look, W. Kim, Z. Fan, A. Botchkarev and H. Morkoç, Appl. Phys. Lett. 72, 2277 (1998).
[42] P. Ferrandis, M. Charles, C. Gillot, R. Escoffier, E. Morvan, A. Torres and G. Reimbold, Microelectron. Eng. 178, 158 (2017).
[43] M. El-Khatib, P. Ferrandis, E. Morvan, G. Guillot, and G. Bremond, Proc. SPIE 10532, 1053225 (2018).
[44] P. Ferrandis, M. El-Khatib, M.-A. Jaud, E. Morvan, M. Charles, G. Guillot and G. Bremond, J. Appl. Phys. 125, 035702 (2019).
[45] P. Ferrandis, M. El-Khatib, M.-A. Jaud, E. Morvan, M. Charles, G. Guillot and G. Bremond, Semicond. Sci. Technol. 34, 045011 (2019).
[46] S. Sudharsanan, and S. Karmalkar, J. Appl. Phys. 107, 064501 (2010).
[47] C. D. Wang, L. S. Yu, S. S. Lau, E. T. Yu, W. Kim, A. E. Botchkarev and H. Morkoç, Appl. Phys. Lett. 72, 1211 (1998).
[48] Z.-Q. Fang, D. C. Look, P. Visconti, D.-F. Wang, C.-Z. Lu, F. Yun, H. Morkoç, S. S. Park and K. Y. Lee, Appl. Phys. Lett. 78, 2178 (2001).
[49] S. Chen, U. Honda, T. Shibata, T. Matsumura, Y. Tokuda, K. Ishikawa, M. Hori, H. Ueda, T. Uesugi and T. Kachi, J. Appl. Phys. 112, 053513 (2012).